Actin-like protein 6A is a novel prognostic indicator promoting invasion and metastasis in osteosarcoma

WEI SUN[1], WANCHUN WANG[1], JIAN LEI[2], HUI LI[1] and YI WU[1]

[1]Department of Orthopedics Surgery, The Second Xiangya Hospital, Central South University, Changsha, Hunan 410011; [2]Department of Pathology, The Affiliated Cancer Hospital of Xiangya School of Medicine, Central South University, Changsha, Hunan 410013, P.R. China

Abstract. Osteosarcoma harbors highly metastatic properties, accounting for postoperative recurrence and metastasis. Actin-like protein 6A (ACTL6A) regulates cell proliferation, migration and differentiation. However, the biologic role of ACTL6A in osteosarcoma remains unknown. In this study, the results showed that, by analysis of frozen fresh primary tumor tissues, matched non-cancerous bone tissues (NCBTs) and biopsy lung metastatic nodule tissues from 30 osteosarcoma patients after radical surgical resection, ACTL6A was overexpressed in osteosarcoma tissues compared with matched NCBTs, and its expression level was associated with osteosarcoma metastasis. Immunohistochemical analyses of osteosarcoma tissue samples from two independent cohorts of formaldehyde-fixed, paraffin-embedded osteosarcoma tissue samples from total of 186 osteosarcoma patients showed that high ACTL6A expression correlated with malignant clinicopathological features such as larger tumor size, high Ennecking grade, high histologic grade, and advanced tumor node metastasis stage. High ACTL6A expression was associated with poor prognosis for patients with osteosarcoma, and an independent and significant risk factor for disease-free survival and overall survival after radical tumor resection. Both *in vitro* and *in vivo* assays showed that ACTL6A overexpression promoted osteosarcoma cell invasion and metastasis, whereas knockdown of ACTL6A expression reduced osteosarcoma cell malignant behavior such as invasion and metastasis. Furthermore, we proved that ACTL6A promoted osteosarcoma cells of metastasis through facilitating epithelial-mesenchymal transition (EMT). In conclusion, data from the present study demonstrated that ACTL6A was associated with poor survival and promoted osteosarcoma cell metastasis through EMT, suggesting that ACTL6A may be a novel prognostic biomarker and therapeutic target for osteosarcoma.

Introduction

Osteosarcoma, the most prevalent bone malignancy, occurred frequently in children and adolescents (1). The survival of osteosarcoma patients is dependent on the clinical stage of the tumor and whether there is lung metastasis (2). For example, osteosarcoma without lung metastasis has an ideal prognosis, with 5-year overall survival (OS) rate range from 20 to 70% after radical tumor resection, whereas osteosarcoma with lung metastasis had an ~20% five-year OS rate (3,4). Despite markedly improved diagnostic and treatment strategies, recurrence and metastasis, especially lung metastasis, is the main obstacle for the long-term survival of osteosarcoma (5). Previous studies reported that changes in gene expression patterns were the main cause of osteosarcoma metastasis (6), and identified a number of some critical metastasis-associated genes, such as p53 and Rb (7,8). To date, the mechanism of osteosarcoma metastasis remains elusive. Thus, it is urgently required to elucidate the mechanisms underlying metastasis of osteosarcoma which will help research on novel strategies for better treatment, biomarkers for prognosis prediction.

Osteosarcoma metastasis is frequent to the lung via the bloodstream, which is involved in multiple biological changes of tumor cells, including cell proliferation, migration, invasion, enabling tumor cells to invade into the vessels and escape from the vessels to form a metastatic nodule in distant organs (9). Recently, substantial evidence also indicate epithelial-mesenchymal transition (EMT), a normal biologic process that enables an epithelial cell change into a mesenchymal cell phenotype, is involved in the metastasis of osteosarcoma (10,11). Actin-like protein 6A (ACTL6A), which is a core 53 kDa subunit of the BRG1/BRM-associated factor complex, involved in diverse cellular processes, such as vesicular transport, spindle orientation, nuclear migration and chromatin remodeling (12,13). ACTL6A is essential for neural progenitor cell proliferation, differentiation and migration during gastrulation (14). ACTL6A is a subunit of the SWI/SNF ATP-dependent chromatin-remodeling complex, which also functions in osteoblast differentiation (15). It was also reported that ACTL6A could suppress epidermal differentiation and

Correspondence to: Dr Yi Wu, Department of Orthopaedics Surgery, The Second Xiangya Hospital, Central South University, Changsha, Hunan 410011, P.R. China
E-mail: wuyi.8@163.com

maintain the progenitor state (16). The conditional knockout of ACTL6A led to terminal differentiation of the epidermis, whereas the ectopic expression of ACTL6A enhanced and maintained the progenitor state of the epidermis (16), indicating that ACTL6A was involved in EMT. Intriguingly, ACTL6A has been identified as a transcriptional regulator and driving pathways that are of specific benefit to the malignant elements within the tumor (17,18). These pathways facilitate cell adhesion, proliferation, migration and invasion (19). The above data indicate the oncogenic role of ACTL6A in osteosarcoma. However, the expression and clinical significance of ACTL6A in osteosarcoma it is still unknown.

In this study, we assessed the ACTL6A expression in osteosarcoma tissues, and the association of ACTL6A expression with clinicopathological features and prognosis of osteosarcoma patients. Then we explored the role of ACTL6A in osteosarcoma by *in vitro* and *in vivo* assays, expecting to provide insightful information for identifying ACTL6A is a novel biomarker to predict the survival of osteosarcoma patients and exploring ACTL6A as a potential target for osteosarcoma.

Materials and methods

Patients and tissue specimens. Three independent cohorts of osteosarcoma samples totaling 216 osteosarcoma patients from two medical institutions were enrolled in this study. Firstly, 30 pairs of frozen fresh primary tumor tissues (PTs), matched non-cancerous bone tissues (NCBTs) and five biopsy lung metastatic nodule tissues from osteosarcoma patients after radical surgical resection were collected from the Department of Orthopedic Surgery, the Second Xiangya Hospital, Central South University (Hunan, China) between January 2009 and December 2010. These tissue samples (screening cohort) were used to screen the expression of ACTL6A mRNA and protein. Another two independent cohorts of formaldehyde-fixed, paraffin-embedded osteosarcoma tissue samples from 186 osteosarcoma patients with radical surgical resection including training cohort (n=110) and validation cohort (n=76) were randomly collected from Department of Orthopedics Surgery, the Second Xiangya Hospital and the Affiliated Cancer Hospital of Xiangya School of Medicine, Central South University, respectively, between June 2007 and April 2010. All patients were pathologically diagnosed with osteosarcoma according to the WHO bone tumor diagnosis criteria and staging system. Data of clinical and pathological variables were also collected for analysis. Prior informed consent was obtained and the study protocol was approved by the Ethics Committee of Xiangya School of Medicine, Central South University.

Patient follow-up. All osteosarcoma patients received regular follow-up by the experienced medical staff in these two hospitals. The follow-up period was defined as the interval between the date of operation and that of the patient's death or the last follow-up. All patients had a mean follow-up time of 63 months (ranging from 8 to 107 months). Recurrence and metastasis were monitored and diagnosed by using clinical examination, ALP levels, computed tomography (CT) or magnetic resonance imaging (MRI) at a three-month interval.

OS was defined as the time interval between tumor resection and death or the last follow-up. Patients alive at the end of follow-up or dead from causes without sign of recurrence were censored. Disease-free survival (DFS) was calculated from tumor resection to the first radiological evidence of metastasis or/and recurrence or biopsies with histologically confirmed metastasis or/and recurrence.

Cell lines and cell culture. The human fetal osteoblastic cell line hFOB 1.19, and three human osteosarcoma cell lines MG-63, U2-OS and SAOS-2 were obtained from the American Type Culture Collection (ATCC, Manassas, VA, USA) and cultured in RPMI-1640 medium (Gibco-BRL, Gaithersburg, MD, USA) supplemented with 10% fetal bovine serum (FBS; HyClone, Logan, UT, USA) in a humidified incubator with 5% CO_2 at 37˚C.

Quantitative real-time polymerase chain reaction (qRT-PCR). Total RNA was isolated from fresh osteosarcoma tissue samples and cell lines by using a TRIzol® reagent (Invitrogen Life Technologies, Carlsbad, CA, USA) according to the manufacturer's instructions. After quantification using a spectrophotometer (Shimadzu, Kyoto, Japan), RNA samples were reversely transcribed into cDNA using a universal cDNA synthesis kit (Toyobo, Osaka, Japan). The cDNA was subjected to qRT-PCR using the SYBR-Green PCR kit (Toyobo) and the assay was performed on an PRISM 7300 Sequence Detection System (Applied Biosystems, Foster City, CA, USA). The PCR cycling parameters were as follows: 50 cycles of 95˚C for 5 sec and 60˚C for 20 sec. The primers for ACTL6A were used as follows: sense, 5'-CCAGGTCTCTATGGCAGTG TAA-3' and antisense, 5'-CGTAAGGTGACAAAAGGAAG GTA-3'; the primers for GAPDH: sense, 5'-CCACCCATGG CAAATTCC-3' and antisense, 5'-GATGGGATTTCCATTG ATGACA-3'. The relative levels of mRNA expression were calculated using the $2^{-\Delta\Delta Ct}$ method based on the threshold cycle (Ct) values and then normalized to the internal control of GAPDH. All the assays were performed in triplicate.

Western blot analysis. Total cellular or tissue protein was extracted by RIPA lysis buffer. The protein concentrations of the lysates were determined according to the bicinchoninic acid (BCA) method using a protein assay kit (Pierce Biotechnology, Inc., Rockford, IL, USA). Cell or tissue lysates containing 100 μg proteins were separated by sodium dodecyl sulfate-polyacrylamide gel electrophoresis (SDS-PAGE) and then transferred onto PVDF membranes (Millipore, Billerica, MA, USA). The PVDF membranes were then blocked by a 5% skim milk solution for 30 min and incubated primary antibody ACTL6A, E-cadherin and N-cadherin (all from Santa Cruz Biotechnology, Inc., Santa Cruz, CA, USA), Snail (Abcam, Cambridge, MA, USA), Twist-1 and vimentin (both from Santa Cruz Biotechnology, Inc.). Membranes were subsequently incubated with an HRP-conjugated secondary antibody (KPL, Gaithersburg, MD, USA). After this, the membranes were subjected to an enhanced chemiluminescence reagent (Thermo Fisher Scientific, Inc., Waltham, MA, USA) and exposed to x-films to detect protein bands. The β-actin antibody (Sigma-Aldrich, St. Louis, MO, USA) was used as a loading control. Protein expression was quantified

by BandScan software (Bio-Rad Laboratories, Inc., Hercules, CA, USA) and defined as the ratio of target protein relative to β-actin.

Immunohistochemistry. Paraffin-embedded tissues were cut into 4-μm sections, and then 4-μm sections deparaffinized and rehydrated. After antigen retrieval by heat-induced epitopes in the 1 mM, pH 8.0 EDTA buffer (Zhongshan Golden Bridge Biotechnology Co., Shanghai, China) for 20 min, endogenous peroxidases of tissue were blocked for 20 min using 0.3% H_2O_2 (Zhongshan Golden Bridge Biotechnology Co.) and then incubated with primary antibody ACTL6A (1:200 dilution; Santa Cruz Biotechnology, Inc.) at 4˚C overnight. The next day, the sections were incubated with horseradish peroxidase-labeled secondary antibody (Zhongshan Golden Bridge Biotechnology Co.) after washing with phosphate-buffered saline (PBS). Subsequently, the sections were counterstained with hematoxylin solution (Zhongshan Golden Bridge Biotechnology Co.) and mounted with a coverslip. The immunohistochemical score of ACTL6A was calculated according to the percentage of positive tumor cells. The percentage of positive staining was defined as follow: 0, <5% positive cells; 1, 5-30% positive cells; 2, 31–50% positive cells; 3, 51-80% positive cells; and 4, >80% positive cells (20). Based on the protein expression, osteosarcoma tissue specimens were divided into the low-expression group (0-1) and high-expression group (≥2) for data analysis.

Vector construction and stable transfection. ACTL6A-knockdown plasmids carrying short hairpin RNAs (shRNA) for ACTL6A (shACTL6A), ACTL6A-expressing plasmid carrying ACTL6A expression vector inserted with ACTL6A coding sequences (CDSs) and its negative control were purchased from GeneChem (Shanghai, China). The sequences of the three shRNAs used to knockdown ACTL6A expression were as follows: ACTL6A-shRNA-1, 5'-TCCAAGTATGCGGTTG AAA-3'; ACTL6A-shRNA-2, 5'-GTACTTCAAGTGTCAG ATT-3'; ACTL6A-shRNA-3, 5'-GGGATAGTTTCCAAGC TAT-3'.

MG-63 cells used for this study were transfected with shACTL6A, ACTL6A expressing or negative control plasmids. Briefly, exponentially growing MG-63 cells were transfected with plasmids using Lipofectamine 2000 (Invitrogen Life Technologies) according to manufacturer's instructions. Cells transfected with negative controls were used as controls. The cells were selected with 3 μg/ml puromycin (Invitrogen Life Technologies) to obtain the stable cell population. Then, the ACTL6A-knockdown efficiency of three shRNAs, ACTL6A overexpression was validated by qRT-PCR and western blot analysis.

3-(4,5-Dimethylthiazol-2-yl)-2,5-diphenyltetrazolium bromide (MTT) assay. MTT assays were used to determine the level of cell proliferation. Cells (5x10³) were seeded into each well of 96-well plates and incubated in a humidified incubator with 5% CO_2 at 37˚C. Three wells of each group were detected every day for up to 7 days. Fresh medium (100 μl) containing 0.5 mg/ml MTT (Sigma-Aldrich) was added to each well and incubated at 37˚C for 4 h. The culture medium was then replaced with 100 μl of dimethyl sulfoxide (DMSO) (Sigma-Aldrich) and incubated at room temperature for 10 min. The optical density of the cells

was measured at 570 nm using a spectrophotometer (BioTek Instruments, Inc., Winooski, VT, USA). The experiments were repeated at least three times.

Wound healing assay. Wound healing assays were used to assess the cell migration capacity (21,22). MG-63 cells with ACTL6A-knockdown, overexpression or control were grown in RPMI-1640 medium with 10% FBS to reach ~90% confluence. Cells were incubate with 10 μg/ml puromycin for 1 h, and then rinsed with ice-cold PBS, and then further cultured in serum-free medium for 24 h. Then, three separate parallel wounds were created using a sterile 10 μl pipette tip and then rinsed with ice-cold PBS. The wound closure was recorded after 24 h. The experiment was performed in triplicate.

Transwell assay. Transwell assays were performed to analyze the cell invasion capacity (23). Briefly, the cells at a density of 1x10⁵ in RPMI-1640 containing 0.1% bovine serum albumin (BSA) were seeded into the upper chambers of Transwell insert precoated with Matrigel (BD Biosciences, San Jose, CA, USA), while the bottom chambers were filled with 200 μl of RPMI-1640 containing 10% FBS. The cells were cultured at 37˚C for 24 h. The cells remaining in the upper chamber were removed using a cotton swap. After fixing with 20% methanol and staining with a solution containing 0.1% crystal violet (Beyotime Institute of Biotechnology, Beijing, China), the number of cells invading into the lower membrane of the inserts was counted and imaged using an inverted fluorescence microscope TE-2000S (Nikon, Tokyo, Japan). For each experiment group, the assay was performed in triplicate, and five random fields of each replicate were chosen for analysis.

Immunofluorescence analysis. Immunofluorescence analysis was used to analyze the effect of ACTL6A on actin cytoskeleton of osteosarcoma cells. To allow direct fluorescence of actin cytoskeleton, the cells were stained with 0.25 mM tetramethylrhodamine isothiocyanate (TRITC)-conjugated phalloidin (Sigma-Aldrich). Nuclei were visualized with 4',6-diamidino-2-phenylindole (DAPI). The slides were imaged by an inverted fluorescence microscope TE-2000S (Nikon).

In vivo metastatic assays. The animal study was approved by the Institutional Animal Care and Use Committee (IACUC) of The Second Xiangya Hospital, Central South University. The animal experiments were performed in accordance with standard IACUC procedures. In briefly, 4-week-old BALB/c nude mice were obtained from Medical Animal Research Institute, Central South University and used to assay the metastatic potential of osteosarcoma cells. MG-63 cells (5x10⁶) of each group were suspended in 0.1 ml of saline and injected into the tail vein of each mouse (n=6). After 30 days, the animals were sacrificed and autopsied. Lung tissue of each mouse was harvested and then fixed in 10% buffered formalin, embedded in paraffin, serially sectioned, and then stained with hematoxylin and eosin (H&E). The number of lung tumor metastatic nodules was counted under the microscope (Nikon).

Statistical analysis. All statistical analyses were performed using SPSS 18.0 statistical software (SPSS Inc., Chicago, IL,
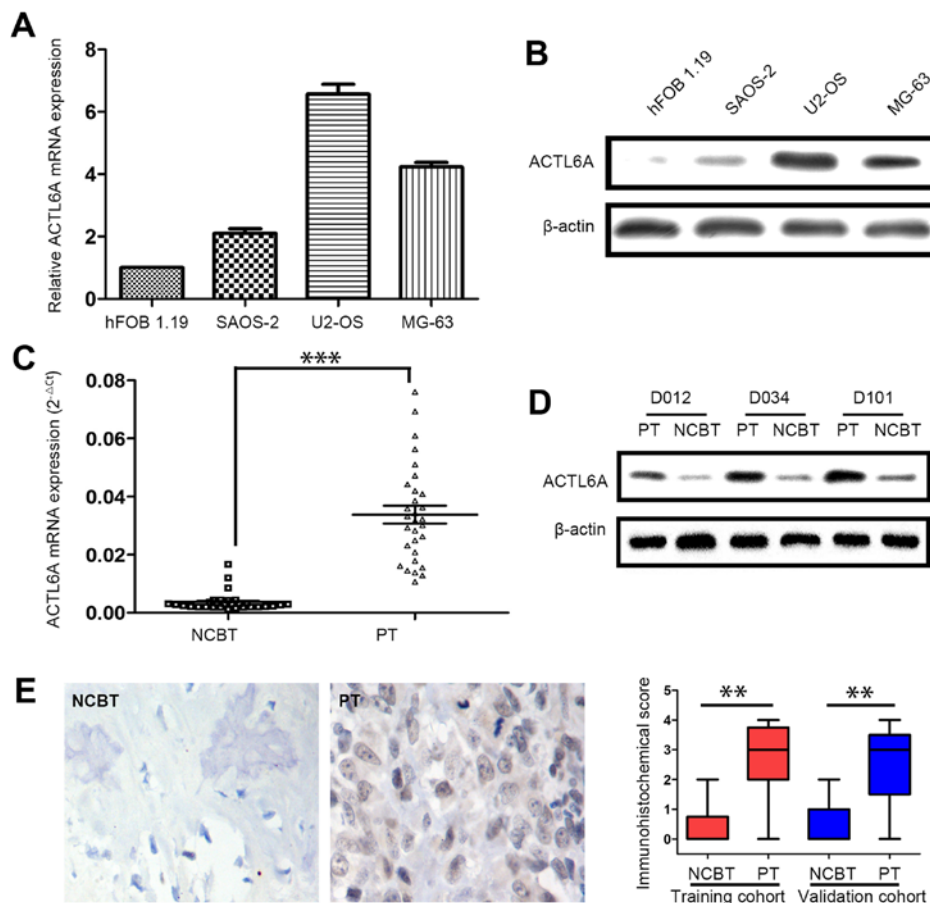
Figure 1. ACTL6A is overexpressed in human osteosarcoma tissues and cell lines. (A and B) ACTL6A was overexpressed in osteosarcoma cell lines. Compared to hFOB 1.19, osteosarcoma cell lines SAOS-2, U2-OS and MG-63 expressed high levels of ACTL6A analyzed by (A) qRT-PCR and (B) western blot analysis. (C and D) ACTL6A was overexpressed in osteosarcoma tumor tissues (n=30). (C) qRT-PCR showed the mRNA expression level of ACTL6A in PTs was higher than in corresponding NCBT. (D) Representative images of western blot analysis. Results showed the protein expression level of ACTL6A in PTs was higher than in corresponding NCBTs. (E) IHC images of ACTL6A protein staining in osteosarcoma tissues. PTs exhibited higher ACTL6A protein expression than corresponding NCBT. Magnification, x400. **P<0.01, ***P<0.001. ACTL6A, actin-like protein 6A; PT, primary tumor tissue; NCBT, non-canerous bone tissue.

USA). Categorical data were analyzed using Fisher's exact test. Continuous data were summarized as mean ± SD and analyzed by using an independent t-test when the variance was homogeneous, or a Mann-Whitney U test if the variance was not homogeneous. OS and DFS curves were plotted using the Kaplan-Meier method and compared by the log-rank test. The univariate and multivariate Cox proportional hazards regression model was used to identify independent predictors for OS and DFS. All tests were two-tailed and P<0.05 was considered statistically significant.

Results

ACTL6A is overexpressed in human osteosarcoma tissues and cell lines. Firstly, the level of ACTL6A expression was assessed in osteosarcoma cell lines by qRT-PCR and western blot analysis. Data showed that, compared to the normal cell line hFOB 1.19, ACTL6A mRNA was overexpressed in osteosarcoma cell lines by qRT-PCR (Fig. 1A). Western blot analysis also showed ACTL6A protein was highly expressed in osteosarcoma cell lines (Fig. 1B). Next, we screened the ACTL6A expression in 30 pairs of fresh osteosarcoma tissues in screening cohort. Notably, the levels of ACTL6A mRNA and protein were dramatically higher in PTs than in matched non-cancerous bone

tissues (NCBTs) (Fig. 1C and D). Furthermore, immunohistochemical (IHC) analysis also showed the expression of ACTL6 protein was significantly higher in PT than in NCBTs from training and validation cohort (Fig. 1E).

ACTL6A overexpression is associated with osteosarcoma metastasis. Then, we analyzed ACTL6A expression among 30 different fresh PTs. Interestingly, ACTL6A expression was higher in PTs of tumor node metastasis (TNM) stage III than that of TNM stage I/II (Fig. 2A). Additionally, ACTL6A expression was much higher in PTs from patients who developed metastases and/or recurrence than those who did not (Fig. 2B). Importantly, ACTL6A expression was higher in lung metastatic nodules (LMNs) than in their corresponding PTs and NCBTs from same patients (n=5) and the ACTL6A expression exhibited the gradient increase from NCBTs, PTs to LMN (Fig. 2C and D). Taken together, these data indicate that ACTL6A may contribute to osteosarcoma progression and metastasis.

Association of ACTL6A expression with clinicopathological characteristics in osteosarcoma patients. Further, IHC was used to detect the ACTL6A expression in osteosarcoma samples from two cohorts of patients including training cohort (n=110) and validation cohort (n=76). Detail
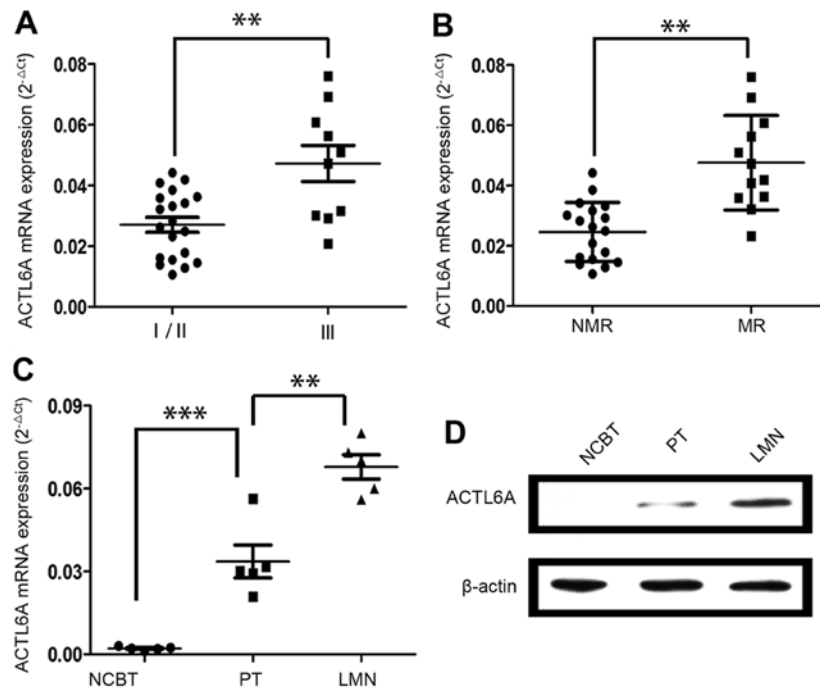
Figure 2. ACTL6A overexpression is associated with osteosarcoma metastasis. (A) ACTL6A expression was higher in PTs at TNM stage III than in those at TNM stage I/II. (B) ACTL6A expression was much higher in PTs from patients who developed metastases or recurrence than those who did not. MR, with metastases or recurrence; NMR, without metastases or recurrence. (C and D) ACTL6A expression in LMNs, PTs and their corresponding NCBTs from the same patient (n=5). (C) ACTL6A mRNA expression exhibited the gradient increase from NCBTs, PTs to LMNs. (D) Representative images of western blot analysis. Results showed the ACTL6A protein expression exhibited the gradient increase from NCBTs, PTs to LMNs. **P<0.01, ***P<0.001. ACTL6A, actin-like protein 6A; TNM, tumor node metastasis; PTs, primary tumor tissues; LMNs, lung metastatic nodules; NCBTs, non-canerous bone tissues.
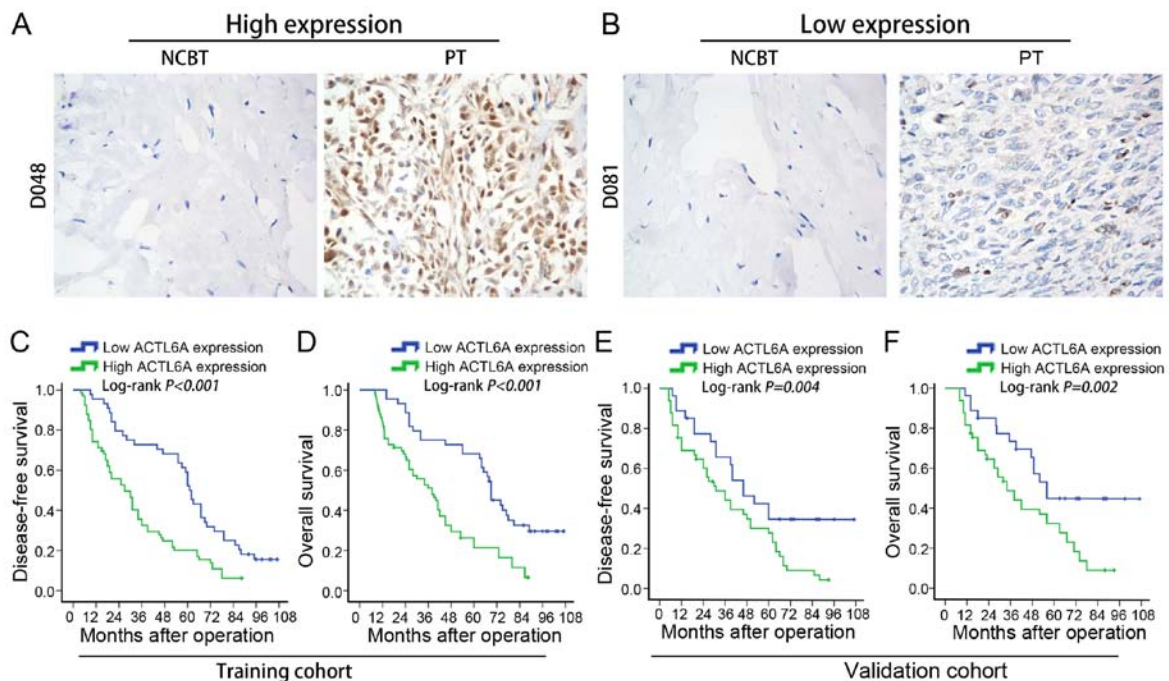

Figure 3. ACTL6A overexpression is associated with poor prognosis of osteosarcoma patients. (A and B) Representative images of osteosarcoma tissues with different ACTL6A protein staining. According to IHC immnostaining score, osteosarcoma patients dichotomized into high ACTL6A expression group (≥2, A) and low ACTL6A expression group (<2, B). (C) Kaplan-Meier survival curves of DFS and (D) OS in training cohort. Log-rank test showed that osteosarcoma patients with high ACTL6A expression had significantly shorter DFS and OS than those with low ACTL6A expression. (E and F) Kaplan-Meier survival curves of (E) DFS and (F) OS in validation cohort. Log-rank test showed that osteosarcoma patients with high ACTL6A expression had significantly shorter DFS and OS than those with low ACTL6A expression. ACTL6A, actin-like protein 6A; DFS, disease-free survival; OS, overall survival.

demographics and clinicopathological characteristics of two cohorts of patients are described in the Table I. In training cohort, patients were divided into two groups, the high ACTL6A expression (Fig. 3A) and the low ACTL6A expression (Fig. 3B)

based on ACTL6A expression. We found that 60.0% (66/110) of PTs exhibited high ACTL6A expression, as compared with 10.9% (12/110) in corresponding NCBTs. By analyzing the relationship between the levels of ACTL6A expression in PTs and the clinicopathological characteristics, results showed that high ACTL6A expression was significantly associated with large tumor size (P<0.001), presence of pathological facture (P=0.018), high Ennecking grade (P=0.015), high histologic grade (P<0.006) and advanced TNM stage (P=0.005). However, it was not associated with patient gender (P=0.676), age (P=0.275), anatomical localization of tumor (P=0.843) or ALP level (P=0.525) (Table II).

Furthermore, we then confirmed the results in validation cohort of 76 osteosarcoma patients. Our data showed that ACTL6A protein was overexpressed in 64.5% (49/76) of PTs, as compared with 13.2% (10/76) in corresponding NCBTs by IHC. High ACTL6A expression was significantly associated with large tumor size (P=0.003), presence of pathological facture (P=0.030), high Ennecking grade (P=0.022), high histologic grade (P=0.008) and advanced TNM stage (P=0.014), whereas it was not associated with patient gender (P=0.890), age (P=0.621), anatomical localization of tumor (P=0.302) or ALP level (P=0.281) (Table II).

High ACTL6A expression level correlated with poor prognosis of osteosarcoma patients. To evaluate the prognostic potential of ACTL6A expression in osteosarcoma tissues, we compared the DFS and OS between patients with high ACTL6A expression and those with low ACTL6A expression. In training cohort, we found that patients with high ACTL6A expression had a shorter DFS (P<0.001; Fig. 3C) and had a shorter OS (P<0.001; Fig. 3D) than those with low ACTL6A expression. To determine whether ACTL6A expression was an independent prognostic factor for osteosarcoma, a univariate analysis was first performed followed by a subsequent multivariate Cox proportional hazards analyses. Remarkably, high ACTL6A expression was found to be a significant and independent predictor for DFS (HR: 3.409, 95% CI: 2.113-5.500, P=0.004; Table III) and OS (HR: 3.602, 95% CI: 2.021-6.420, P=0.006; Table III) in osteosarcoma.

Furthermore, we confirmed the correlation between ACTL6A expression level and osteosarcoma prognosis in validation cohort and also found that osteosarcoma patients with high ACTL6A expression had a worse DFS (P=0.004; Fig. 3E) and a worse OS (P=0.002; Fig. 3F) than those with low ACTL6A expression. Multivariate Cox regression analysis also showed that high ACTL6A expression was an independent predictor for DFS (HR: 2.718, 95% CI: 1.514-4.879, P=0.010; Table IV) and OS (HR: 2.834, 95% CI: 2.006-4.003, P=0.013; Table IV). Above of all, these data suggest that high ACTL6A expression predicts poor prognosis in osteosarcoma patients and may contribute to the metastasis of osteosarcoma.

ACTL6A enhances invasion and metastasis of osteosarcoma cells in vitro and in vivo. To determine the roles of ACTL6A in osteosarcoma invasion and metastasis, we established ACTL6A overexpression cell line MG-63[ACTL6A], ACTL6A-knockdown cell line MG-63[shACTL6A] and its control cell line MG-63[Control] (Fig. 4A-a-b) according to the expression level of ACTL6A in osteosarcoma cell lines and biological characteristics of osteosarcoma cell lines. By wound healing

Table I. Patient demographics and clinicopathological characteristics in the training and validation cohorts.

Variables	Training cohort		Validation cohort		P-value
	n	%	n	%	
Gender					0.314
Male	75	68.2	57	75.0	
Female	35	31.8	19	25.0	
Age (years)					0.319
<45	57	51.8	45	59.2	
>45	53	48.2	31	40.8	
Anatomical site					0.243
Femur/tibia	89	80.9	56	73.7	
Elsewhere	21	19.1	20	26.3	
Tumor size (cm)					0.797
<8	50	45.5	36	47.4	
>8	60	54.5	40	52.6	
ALP level (U/l)					0.800
<150	44	44.0	29	38.2	
>150	66	66.0	47	61.8	
Pathological fracture					0.517
Absent	91	82.7	60	78.9	
Present	19	17.3	16	21.1	
Ennecking grade					0.706
2a	61	55.5	40	52.6	
2b	49	44.5	36	47.4	
Histologic grade					0.220
Low	65	59.1	38	50.0	
High	45	40.9	38	50.0	
TNM stage					0.882
I/II	62	56.4	42	55.3	
III	48	43.6	34	44.7	

assays, we evidenced that overexpression of ACTL6A enhanced MG-63 cell migration, whereas knockdown of ACTL6A dramatically inhibited migration (Fig. 4B-a-b). Transwell invasion assays showed that, compared with MG-63[Control], a significant increase in the number of invaded cells was observed in MG-63[ACTL6A] group, but an obvious decrease in the number of invaded cells was observed in MG-63[shACTL6A] group (Fig. 4C-a-b). Immunofluorescence was used to analyze the cell cytoskeleton by F-actin staining. The results showed that compared to MG-63[Control] and MG-63[shACTL6A] cells showed the stress fiber-like structures disappeared and the morphology regressed to cobble-stone shape, but MG-63[ACTL6A] cells showed obvious reorganization of actin cytoskeleton and the cell appearance changed into more spindle-like, fibroblastic morphology (Fig. 4D). Also, we observed overexpression of ACTL6A significantly accelerated MG-63 cell proliferation, while knockdown of ACTL6A

Table II. Correlations of ACTL6A expression with clinicopathological variables of osteosarcoma in training and validation cohort.

| | | Training cohort | | | | Validation cohort | | |
| | | ACTL6A expression | | | | ACTL6A expression | | |
Variables	N	Low	High	P-value	N	Low	High	P-value
Gender				0.676				0.890
Male	75	31	44		57	20	37	
Female	35	13	22		19	7	12	
Age (years)				0.275				0.621
<45	57	20	37		45	17	28	
>45	53	24	29		31	10	21	
Anatomical site				0.843				0.302
Femur/tibia	89	36	53		56	18	38	
Elsewhere	21	8	13		20	9	11	
Tumor size (cm)				**<0.001**				**0.003**
<8	50	30	20		36	19	17	
>8	60	14	46		40	8	32	
ALP level (U/l)				0.525				0.281
<150	44	16	28		29	14	15	
>150	66	28	38		47	23	24	
Pathological fracture				**0.018**				**0.030**
Absent	91	41	50		60	25	35	
Present	19	3	16		16	2	14	
Ennecking grade				**0.028**				**0.022**
2a	61	30	31		40	19	21	
2b	49	14	35		36	8	28	
Histologic grade				**0.006**				**0.008**
Low	65	33	32		38	19	19	
High	45	11	34		38	8	30	
TNM stage				**0.005**				**0.014**
I/II	62	32	30		42	20	22	
III	48	12	36		34	7	27	

ACTL6A, actin-like protein 6A. Bold text, statistically significant.

dramatically inhibited MG-63 cells proliferation by MTT assays (Fig. 4E). These data support a metastasis-promoting role of ACTL6A in osteosarcoma.

To verify the *in vitro* results, we further evaluated the role of ACTL6A by using an *in vivo* mouse metastasis model. We observed that nude mice injected with MG-63[ACTL6A] cells had a markedly larger size and number of lung metastasis tumor nodules than those injected with MG-63[Control] cells (Fig. 4F-a-b). However, nude mice injected with MG-63[shACTL6A] cells had a smaller size and number of lung metastatic tumors than those injected with MG-63[Control] cells (Fig. 4F-a-b). By *in vitro* and *in vivo* assays, we demonstrated ACTL6A have the potential of enhancing invasion and metastasis of osteosarcoma cells.

ACTL6A enhances metastasis of osteosarcoma by promoting EMT. ACTL6A suppress epidermal differentiation, and maintain the progenitor state (16). Such a phenomenon was associated with EMT in carcinoma cells, an important mechanism on metastasis. Interestingly, knockdown of ACTL6A resulted in the cell appearance with more cobble-like, epithelial morphology and the cell appearance became more spindle-like, fibroblastic morphology when ACTL6A overexpressed in MG-63 cells (Fig. 4D), these suggested that ACTL6A may be associated with EMT. Western blot analysis showed the expression of mesenchymal marker such as Twist-1, Snail, vimentin, and N-cadherin was significantly lower in MG-63[shACTL6A] cells than in MG-63[Control] cells, while the expression of epithelial marker E-cadherin was much higher in MG-63[shACTL6A] than in MG-63[Control] cells. Conversely, relative to MG-63[Control] cells, the expression of mesenchymal marker such as Snail, Twist-1, vimentin and N-cadherin was significantly increased in MG-63[ACTL6A] cells and the

Table III. Univariate and multivariate analysis of DFS and OS in training cohort.

Variables		DFS Univariate analysis HR (95% CI)	P-value	DFS Multivariate analysis HR (95% CI)	P-value	OS Univariate analysis HR (95% CI)	P-value	OS Multivariate analysis HR (95% CI)	P-value
Gender	Male vs. female	1.075 (0.702-1.634)	0.302		NA	1.162 (0.603-2.246)	0.209		NA
Age (years)	<45 vs. >45	0.973 (0.672-1.401)	0.148		NA	0.802 (0.541-1.192)	0.131		NA
Anatomical site	Femur/tibia vs. elsewhere	0.786 (0.514-1.197)	0.153		NA	0.914 (0.635-1.748)	0.206		NA
Tumor size (cm)	<8 vs. >8	2.043 (1.434-2.915)	0.004	1.824 (1.403-2.371)	0.035	1.908 (1.364-2.652)	0.009	1.565 (1.186-2.064)	0.028
ALP level (U/l)	<150 vs. >150	4.252 (2.923-6.181)	<0.001	2.154 (1.731-2.675)	0.019	3.843 (2.324-6.353)	<0.001	2.023 (1.612-2.564)	0.017
Pathological fracture	Absent vs. present	3.063 (1.833-5.114)	0.002	2.034 (1.562-2.642)	0.026	3.301 (2.343-4.654)	0.005	1.914 (1.502-2.431)	0.020
Ennecking grade	2a vs. 2b	1.378 (0.834-2.262)	0.082	1.036 (0.693-1.542)	0.185	1.431 (0.931-2.191)	0.071	1.053 (0.902-1.231)	0.093
Histologic grade	Low vs. high	1.643 (1.011-2.665)	0.045	1.084 (0.762-1.552)	0.064	1.176 (0.913-1.512)	0.105		NA
TNM stage	I/II vs. III	2.972 (2.061-4.283)	0.003	3.213 (2.042-5.051)	0.007	3.082 (2.174-4.369)	0.002	2.401 (1.792-3.217)	0.011
ACTL6A expression	Low vs. high	4.943 (2.925-8.366)	<0.001	3.409 (2.113-5.500)	0.004	4.482 (3.101-6.472)	<0.001	3.602 (2.021-6.420)	0.006

DFS, disease-free survival; OS, overall survival; HR, hazard ratio; CI, confidence interval; TNM, tumor node metastasis; ACTL6A, actin-like protein 6A.

Table IV. Univariate and multivariate analysis of DFS and OS in validation cohort.

Variables		DFS Univariate analysis HR (95% CI)	P-value	DFS Multivariate analysis HR (95% CI)	P-value	OS Univariate analysis HR (95% CI)	P-value	OS Multivariate analysis HR (95% CI)	P-value
Gender	Male vs. female	1.244 (0.741-2.064)	0.401		NA	1.125 (0.672-1.873)	0.148		NA
Age (years)	<45 vs. >45	0.867 (0.573-1.294)	0.109		NA	0.912 (0.673-1.234)	0.126		NA
Anatomical site	Femur/tibia vs. elsewhere	0.782 (0.531-1.143)	0.130		NA	0.773 (0.514-1.165)	0.153		NA
Tumor size (cm)	<8 vs. >8	3.802 (2.071-4.584)	<0.001	2.603 (1.815-3.186)	0.017	2.643 (1.871-3.722)	0.009	1.794 (1.247-2.581)	0.036
ALP level (U/l)	<150 vs. >150	2.715 (1.682-4.372)	0.007	2.525 (1.503-4.232)	0.023	3.434 (2.311-5.094)	0.004	2.396 (1.523-3.752)	0.016
Pathological fracture	Absent vs. present	4.013 (2.782-5.786)	<0.001	3.046 (2.017-4.593)	<0.001	3.644 (2.383-5.562)	<0.001	2.632 (1.947-3.572)	0.005
Ennecking grade	2a vs. 2b	1.205 (1.051-1.372)	0.048	1.044 (0.902-1.212)	0.097	1.067 (0.834-1.352)	0.182		NA
Histologic grade	Low vs. high	1.108 (0.914-1.332)	0.104		NA	1.038 (0.724-1.473)	0.207		NA
TNM stage	I/II vs. III	2.601 (1.534-4.410)	0.008	2.149 (1.373-3.344)	0.039	2.847 (1.681-4.850)	0.006	2.437 (1.421-4.297)	0.025
ACTL6A expression	Low vs. high	3.046 (2.293-4.046)	0.004	2.718 (1.514-4.879)	0.010	3.801 (2.412-5.990)	0.002	2.834 (2.006-4.003)	0.013

DFS, disease-free survival; OS, overall survival; HR, hazard ratio; CI, confidence interval; TNM, tumor node metastasis; ACTL6A, actin-like protein 6A.
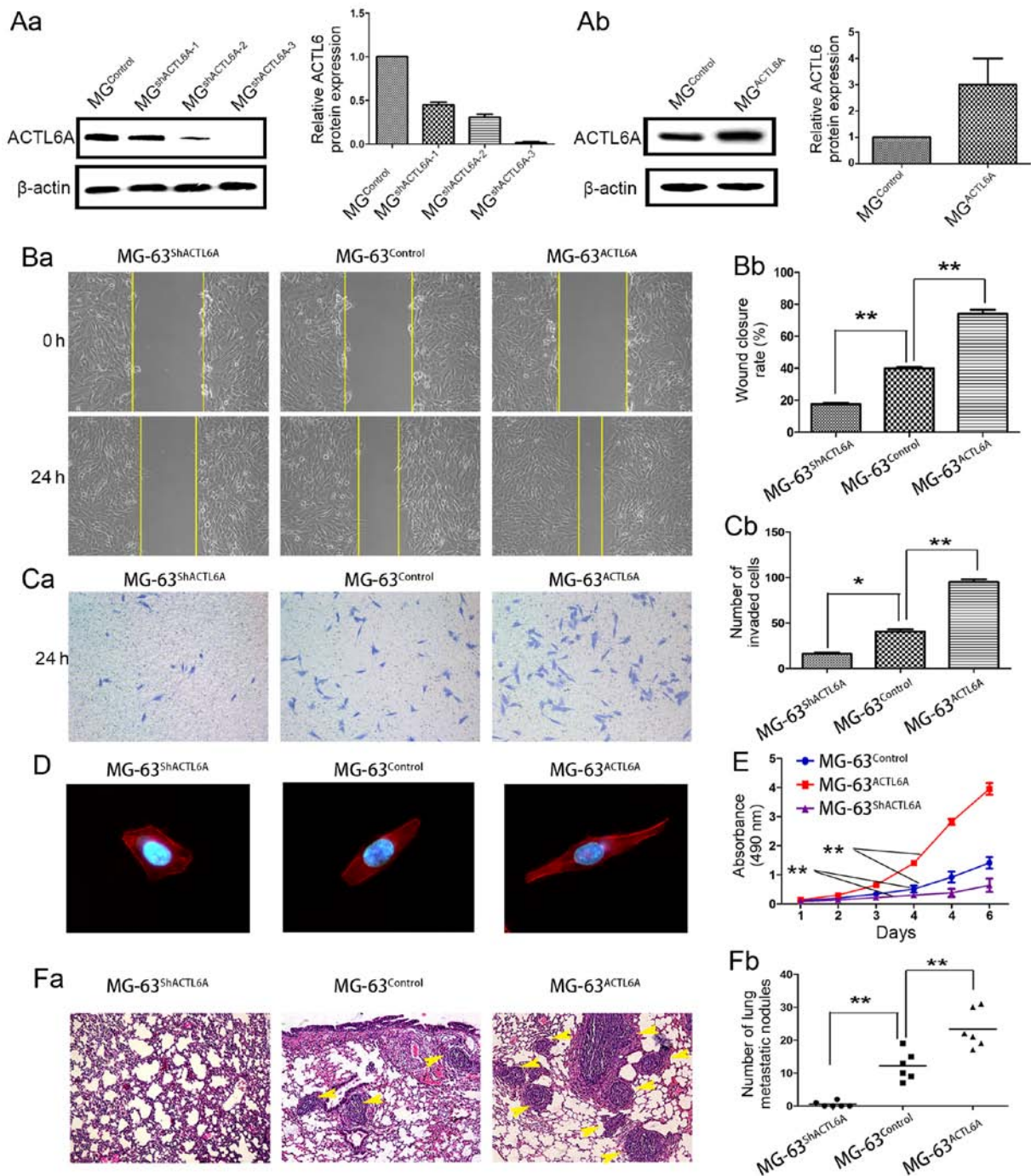
Figure 4. ACTL6A promotes invasion and metastasis of osteosarcoma cells *in vitro* and *in vivo*. (A) ACTL6A overexpression and knockdown cells were stably established. (A-a) MG-63 osteosarcoma cells were stably transfected with shRNA plasmids and (A-b) ACTL6A-expressing plasmids, and then subjected to analysis of ACTL6A expression by western blot analysis. (B-a-b) Wound healing assays showed ACTL6A promoted migration of osteosarcoma cells. (B-a) Representative micrographs of wound healing assays in each group. (B-b) The rate of wound healing in each group was calculated and compared. Results showed ACTL6A-overexpression in osteosarcoma cells MG-63[ACTL6A] exhibited a faster wound healing capacity than control cells MG-63[Control], whereas ACTL6A-knockdown osteosarcoma cells MG-63[shACTL6A] showed lower closure than control cells MG-63[Control]. (C-a-b) Transwell invasion assays showed that ACTL6A enhanced invasion of osteosarcoma cells. (C-a) Representative micrographs of Transwell assays in each group. (C-b) The number of invaded cells in each group was calculated and compared. Results showed that ACTL6A-overexpression MG-63 cells MG-63[ACTL6A] exhibited increase in invasion compared with control cells MG-63[Control]. In contrast, ACTL6A-knockdown MG-63 cells MG-63[shACTL6A] showed decrease in invasion compared with control cells MG-63[Control]. (D) ACTL6A affected cell morphological changes of osteosarcoma cells. Immunofluorescence was used to analyze the morphological changes of MG-63 cells infected with plasmids expressing ACTL6A shRNA, ACTL6A and its negative control. F-actin filaments were visualized in cells using rhodamine-phalloidin. (E) MTT was used to assay the proliferation ability of MG-63[ACTL6A], MG-63[shACTL6A] and MG-63[Control] cells. (F-a-b) ACTL6A enhanced osteosarcoma cell metastasis *in vivo*. (F-a) Representative images of lung metastasis, (F-b) the number of lung metastatic nodules was calculated and compared. Magnification, x100. *P<0.05, **P<0.01. Error bar, SD. ACTL6A, actin-like protein 6A; SD, standard deviation.

expression of epithelial marker E-cadherin was highly reduced in MG-63[ACTL6A] cells (Fig. 5A). These indicate that ACTL6A may enhance metastasis of osteosarcoma by facilitating EMT.

Next, to confirm whether ACTL6A promotes invasion and metastasis of hepatocellular carcinoma (HCC) by facilitating EMT, we reintroduced Twist-1 into MG-63[shACTL6A] and
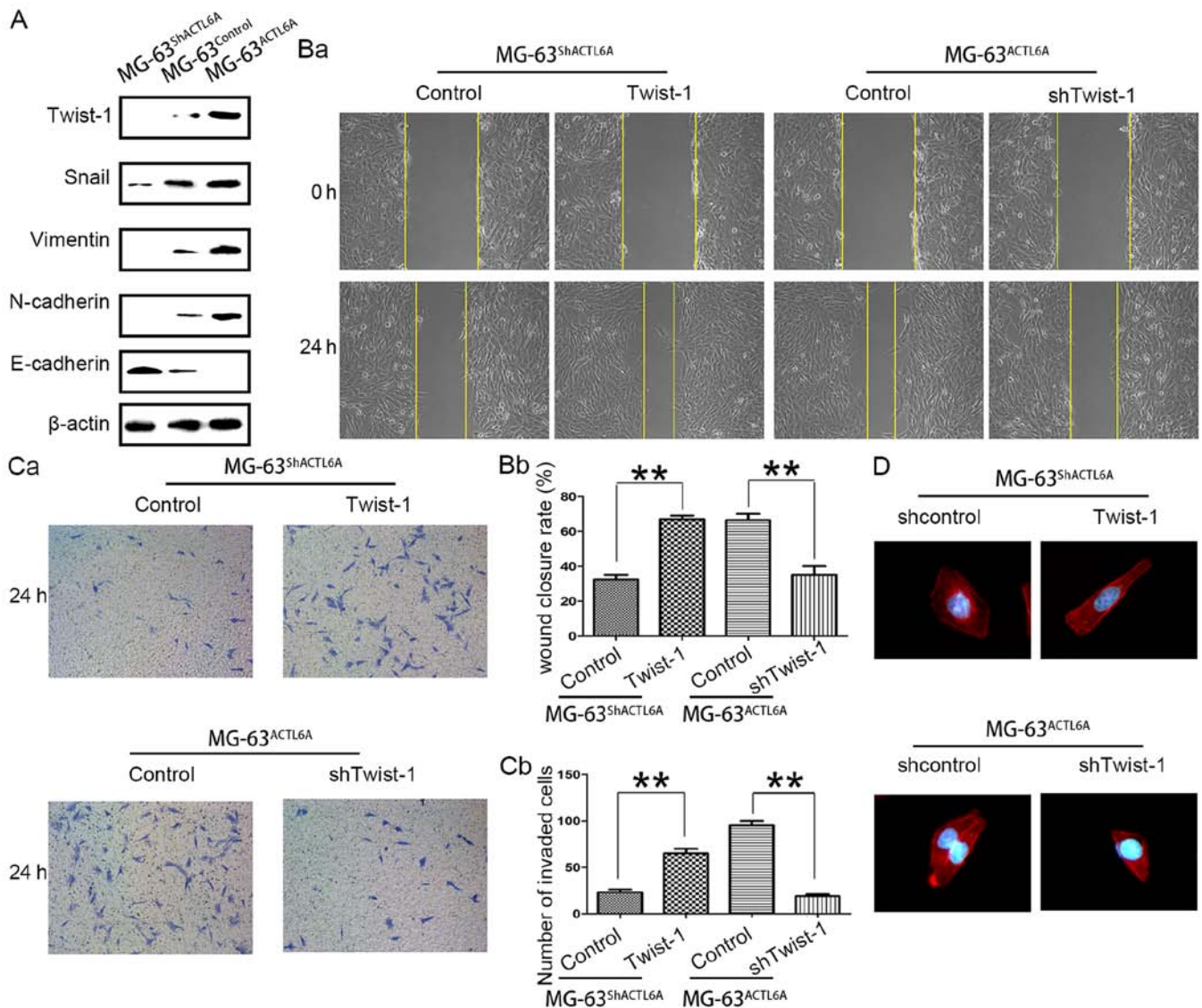
Figure 5. ACTL6A enhances EMT in osteosarcoma. (A) Western blot analysis was employed to detect the expression level of Twist-1, Snail, vimentin, N-cadherin and E-cadherin in MG-63[ACTL6A], MG-63[shACTL6A] and MG-63[Control] cells. (B-a-b) The wound healing assay was used to investigate the changes of migration ability after Twist-1 was reintroduced into MG-63[shACTL6A] cells, and Twist-1 was knockdown in MG-63[ACTL6A] cells. (B-a) Representative micrographs of wound healing assays in each group. (B-b) The rate of wound healing in each group was calculated and compared. (C-a-b) The Transwell assay was used to investigate the changes of invasion ability after Twist-1 was reintroduced into MG-63[shACTL6A] cells, and Twist-1 was knocked down in cells. (C-a) Representative micrographs of Transwell assays in each group. (C-b) The number of invaded cells in each group was calculated and compared. (D) Twist-1 mediated ACTL6A-induced morphological changes of MG-63 cells. Fluorescence images of cells showing reorganization of actin cytoskeleton by staining with TRITC-phalloidin (F-actin) and nuclei with DAPI. **P<0.01. Error bar, SD. ACTL6A, actin-like protein 6A; EMT, epithelial-mesenchymal transition.

knocked down Twist-1 in MG-63[ACTL6A] (data not shown), as Twist-1, a key EMT driver, has been implicated in regulating the osteogenic cell lineage differentiation (24,25). The wound healing assays showed that cells migrated faster after Twist-1 was reintroduced into MG-63[shACTL6A] cells, when downregulation of Twist-1 expression in MG-63[ACTL6A] restrain the ACTL6A-promoted migration (Fig. 5B-a-b). Similarly, the Transwell invasion assays also showed that the numbers of MG-63[shACTL6A] cells passed through the Matrigel was significantly increased after Twist-1 was reintroduced, while the number of MG-63[ACTL6A] passed through the Matrigel was significantly decreased after Twist-1 knockdown (Fig. 5C-a-b). Further, MG-63[shACTL6A] showed the reorganization of actin cytoskeleton and changed the cell appearance to more spindle-like, fibroblastic morphology after Twist-1 was reintroduced, but the stress fiber-like structures disappeared and the morphology regressed to cobble-stone shape in MG-63[ACTL6A] cells after Twist-1 knockdown (Fig. 5D). In all, these studies suggested that ACTL6A could promote osteosarcoma cell metastasis by enhancing EMT.

Discussion

Metastasis, mainly present as pulmonary metastasis, significantly affects the prognosis of osteosarcoma patients (26). The mechanism of osteosarcoma metastasis remains to be determined. ACTL6A, a nuclear actin-related protein (Arp), is a component of a number of chromatin-modifying complexes SWI/SNF and is indispensable for SWI/SNF complex regulation of chromatin structure (27). SWI/SNF, in its role as a

chromatin-remodeling complex and transcription, is a convergent point for signaling from the various hormones, growth factors, and kinase cascades that influence lineage choice in stem cells, especially in an increasing tendency of bone marrow stromal cells (BMSCs) to differentiate into adipocytes at the expense of osteoblasts (15). These biological functions are also involved in oncogenic phenomena, suggesting the possible oncogenic role of ACTL6A in osteosarcoma.

In the present study, we demonstrated that both ACTL6A mRNA and protein levels elevated significantly in osteosarcoma tissues and cell lines. High ACTL6A expression was found to be positively correlated with the metastatic potential of osteosarcoma cells. These suggest ACTL6A may play a role in osteosarcoma metastasis. Further analysis of the association of ACTL6A expression with the clinicopathologic characteristics in osteosarcoma patients of training cohort reveals that ACTL6A overexpression was significantly correlated with malignant clinicopathological variables, including large tumor size, presence of pathological facture, high Enecking grade and high histologic grade. These clinicopathological variables are associated with poor prognosis of the patients with osteosarcoma (28), suggesting ACTL6A expression may be important for the acquirement of malignant potential in osteosarcoma. Moreover, compared with early stage osteosarcoma, ACTL6A expression was also significantly upregulated in tumors in advanced osteosarcoma, suggesting ACTL6A plays an important role in the progression of osteosarcoma. The Kaplan-Meier analysis shows that the osteosarcoma patients with high ACTL6A expression in general had worse prognosis than those with low expression, and multivariable Cox regression analysis indicates that high ACTL6A expression is an independent risk factor for the prognosis of osteosarcoma patients. The validity of ACTL6A to predict osteosarcoma prognosis was validated in validation cohort, suggesting that ACTL6A may be a useful biomarker to predict the survival of osteosarcoma patients as well as the necessity for further study of ACTL6A as a novel target for future control of osteosarcoma. These data also manifest that ACTL6A shows the biological function of metastasis in osteosarcoma.

In vitro experiments were performed to confirm that overexpression of ACTL6A in osteosarcoma cells significantly enhanced cell migration, invasion and proliferation, while knockdown of ACTL6A expression in osteosarcoma cells markedly inhibited cell migration, invasion and proliferation. *In vivo* nude mouse model data of lung metastasis further confirmed that ACTL6A promoted metastasis of osteosarcoma cells. Our data mirrored the biological function of ACTL6A in cell proliferation and migration in developmental biology (14), suggesting that ACTL6A may have a potential role in promotion of tumor metastasis. Our data are novel in osteosarcoma, although also consistent with a recent study showing ACTL6A expression upregulated in HCC tissues and ACTL6A promoted HCC cell proliferation, invasion and metastasis (29).

EMT, enabling the tumor cells to gain invasive and metastatic properties, plays a vital role in the initiation of cancer metastasis (24,30). ACTL6A suppresses epidermal differentiation, and maintains the progenitor state (16), which is associated with EMT. Therefore, it is of interest to investigate whether ACTL6A promotes invasion and metastasis of osteosarcoma

cells by facilitating EMT. Our findings indicate that ACTL6A could modulate the reorganization of F-actin and the formation of stress fiber-like structures. ACTL6A depletion markedly attenuated the expression of mesenchymal markers such as Twist-1, Snail, vimentin and N-cadherin, while increased the expression of epithelial marker E-cadherin. Conversely, ACTL6A overexpression significantly upregulated the expression of mesenchymal markers such as Twist-1, vimentin and N-cadherin, while downregulated the expression of epithelial marker E-cadherin. Twist-1 is a key EMT driver that directly binds to CDH1 promoter and inhibits E-cadherin transcription (31). Analysis of EMT transcription factors Twist-1 in ACTL6A-mediated EMT program found that reintroduced Twist-1 into MG-63[shACTL6A] recover the function of ACTL6A deletion including promoting cell migration, invasion and morphologic changes in cytoskeleton organization. On the contrary, knockdown of Twist-1 in MG-63[ACTL6A] compromised the function induced by ACTL6A overexpression. Our results also provide a link between ACTL6A and Twist-1 in EMT and Twist-1 was the potential target of ACTL6A in osteosarcoma. There was a study proposed that ACTL6A played a pivotal role in supporting the pro-oncogenic functions of Notch1 in EMT (29). Twist-1 also is promoted by the activated Notch1 signaling (32). Available data indicated that ACTL6A may transactivate Twist-1 expression via Notch1 signaling. However, further studies are needed to explore the possible role of ACTL6A in EMT-related signal transduction pathway in osteosarcoma.

In conclusion, the present study showed that ACTL6A overexpression was significantly associated with malignant behavior and poor prognosis of osteosarcoma. Furthermore, we have demonstrated that ACTL6A could promote the metastasis of osteosarcoma via facilitating EMT. Collectively, our data indicate that ACTL6A functions as a potential oncogene and a biomarker to predict prognosis in osteosarcoma, supporting the pursuit of ACTL6A as a prospective therapeutic target for osteosarcoma in clinical practice.

References

1. Mirabello L, Troisi RJ and Savage SA: International osteosarcoma incidence patterns in children and adolescents, middle ages and elderly persons. Int J Cancer 125: 229-234, 2009.
2. Ritter J and Bielack SS: Osteosarcoma. Ann Oncol 21 (Suppl 7): vii320-vii325, 2010.
3. Isakoff MS, Bielack SS, Meltzer P and Gorlick R: Osteosarcoma: current treatment and a collaborative pathway to success. J Clin Oncol 33: 3029-3035, 2015.
4. Klein MJ and Siegal GP: Osteosarcoma: anatomic and histologic variants. Am J Clin Pathol 125: 555-581, 2006.
5. Ren HY, Sun LL, Li HY and Ye ZM: Prognostic significance of serum alkaline phosphatase level in osteosarcoma: a meta-analysis of published data. BioMed Res Int 2015: 160835, 2015.
6. Zhang Y, Zhang L, Zhang G, Li S, Duan J, Cheng J, Ding G, Zhou C, Zhang J, Luo P, *et al*: Osteosarcoma metastasis: prospective role of ezrin. Tumour Biol 35: 5055-5059, 2014.
7. Scott MC, Sarver AL, Tomiyasu H, Cornax I, Van Etten J, Varshney J, O'Sullivan MG, Subramanian S and Modiano JF: Aberrant retinoblastoma (RB)-E2F transcriptional regulation defines molecular phenotypes of osteosarcoma. J Biol Chem 290: 28070-28083, 2015.
8. Del Mare S, Husanie H, Iancu O, Abu-Odeh M, Evangelou K, Lovat F, Volinia S, Gordon J, Amir G, Stein J, *et al*: WWOX and p53 dysregulation synergize to drive the development of osteosarcoma. Cancer Res 76: 6107-6117, 2016.
9. Aguirre-Ghiso JA: Models, mechanisms and clinical evidence for cancer dormancy. Nat Rev Cancer 7: 834-846, 2007.

10. Yang G, Yuan J and Li K: EMT transcription factors: implication in osteosarcoma. Med Oncol 30: 697, 2013.
11. Hou CH, Lin FL, Hou SM and Liu JF: Cyr61 promotes epithelial-mesenchymal transition and tumor metastasis of osteosarcoma by Raf-1/MEK/ERK/Elk-1/TWIST-1 signaling pathway. Mol Cancer 13: 236, 2014.
12. Zhao K, Wang W, Rando OJ, Xue Y, Swiderek K, Kuo A and Crabtree GR: Rapid and phosphoinositol-dependent binding of the SWI/SNF-like BAF complex to chromatin after T lymphocyte receptor signaling. Cell 95: 625-636, 1998.
13. Krasteva V, Buscarlet M, Diaz-Tellez A, Bernard MA, Crabtree GR and Lessard JA: The BAF53a subunit of SWI/SNF-like BAF complexes is essential for hemopoietic stem cell function. Blood 120: 4720-4732, 2012.
14. Lessard J, Wu JI, Ranish JA, Wan M, Winslow MM, Staahl BT, Wu H, Aebersold R, Graef IA and Crabtree GR: An essential switch in subunit composition of a chromatin remodeling complex during neural development. Neuron 55: 201-215, 2007.
15. Nguyen KH, Xu F, Flowers S, Williams EA, Fritton JC and Moran E: SWI/SNF-mediated lineage determination in mesenchymal stem cells confers resistance to osteoporosis. Stem Cells 33: 3028-3038, 2015.
16. Bao X, Tang J, Lopez-Pajares V, Tao S, Qu K, Crabtree GR and Khavari PA: ACTL6a enforces the epidermal progenitor state by suppressing SWI/SNF-dependent induction of KLF4. Cell Stem Cell 12: 193-203, 2013.
17. Lu W, Fang L, Ouyang B, Zhang X, Zhan S, Feng X, Bai Y, Han X, Kim H, He Q, et al: Actl6a protects embryonic stem cells from differentiating into primitive endoderm. Stem Cells 33: 1782-1793, 2015.
18. Park J, Wood MA and Cole MD: BAF53 forms distinct nuclear complexes and functions as a critical c-Myc-interacting nuclear cofactor for oncogenic transformation. Mol Cell Biol 22: 1307-1316, 2002.
19. Zhao D, Pan C, Sun J, Gilbert C, Drews-Elger K, Azzam DJ, Picon-Ruiz M, Kim M, Ullmer W, El-Ashry D, et al: VEGF drives cancer-initiating stem cells through VEGFR-2/Stat3 signaling to upregulate Myc and Sox2. Oncogene 34: 3107-3119, 2015.
20. Yong KJ, Gao C, Lim JS, Yan B, Yang H, Dimitrov T, Kawasaki A, Ong CW, Wong KF, Lee S, et al: Oncofetal gene SALL4 in aggressive hepatocellular carcinoma. N Engl J Med 368: 2266-2276, 2013.
21. Pullar CE, Chen J and Isseroff RR: PP2A activation by beta2-adrenergic receptor agonists: novel regulatory mechanism of keratinocyte migration. J Biol Chem 278: 22555-22562, 2003.
22. Fang F, Chang RM, Yu L, Lei X, Xiao S, Yang H and Yang LY: MicroRNA-188-5p suppresses tumor cell proliferation and metastasis by directly targeting FGF5 in hepatocellular carcinoma. J Hepatol 63: 874-885, 2015.
23. Su S, Liu Q, Chen J, Chen J, Chen F, He C, Huang D, Wu W, Lin L, Huang W, et al: A positive feedback loop between mesenchymal-like cancer cells and macrophages is essential to breast cancer metastasis. Cancer Cell 25: 605-620, 2014.
24. Qiang L and He YY: Autophagy deficiency stabilizes TWIST1 to promote epithelial-mesenchymal transition. Autophagy 10: 1864-1865, 2014.
25. Horvai AE, Roy R, Borys D and O'Donnell RJ: Regulators of skeletal development: a cluster analysis of 206 bone tumors reveals diagnostically useful markers. Mod Pathol 25: 1452-1461, 2012.
26. Kempf-Bielack B, Bielack SS, Jürgens H, Branscheid D, Berdel WE, Exner GU, Göbel U, Helmke K, Jundt G, Kabisch H, et al: Osteosarcoma relapse after combined modality therapy: an analysis of unselected patients in the Cooperative Osteosarcoma Study Group (COSS). J Clin Oncol 23: 559-568, 2005.
27. Lee K, Shim JH, Kang MJ, Kim JH, Ahn JS, Yoo SJ, Kim Kwon Y and Kwon H: Association of BAF53 with mitotic chromosomes. Mol Cells 24: 288-293, 2007.
28. Ferrari S, Bertoni F, Mercuri M, Picci P, Giacomini S, Longhi A and Bacci G: Predictive factors of disease-free survival for non-metastatic osteosarcoma of the extremity: an analysis of 300 patients treated at the Rizzoli Institute. Ann Oncol 12: 1145-1150, 2001.
29. Xiao S, Chang RM, Yang MY, Lei X, Liu X, Gao WB, Xiao JL and Yang LY: Actin-like 6A predicts poor prognosis of hepatocellular carcinoma and promotes metastasis and epithelial-mesenchymal transition. Hepatology 63: 1256-1271, 2016.
30. Thiery JP, Acloque H, Huang RY and Nieto MA: Epithelial-mesenchymal transitions in development and disease. Cell 139: 871-890, 2009.
31. Huang W, Chen Z, Shang X, Tian D, Wang D, Wu K, Fan D and Xia L: Sox12, a direct target of FoxQ1, promotes hepatocellular carcinoma metastasis through up-regulating Twist1 and FGFBP1. Hepatology 61: 1920-1933, 2015.
32. Hsu KW, Hsieh RH, Huang KH, Fen-Yau Li A, Chi CW, Wang TY, Tseng MJ, Wu KJ and Yeh TS: Activation of the Notch1/STAT3/Twist signaling axis promotes gastric cancer progression. Carcinogenesis 33: 1459-1467, 2012.